Concentration-Dependent Thermophoretic Accumulation for the Detection of DNA Using DNA-Functionalized Nanoparticles

ARTICLE *in* ANALYTICAL CHEMISTRY · FEBRUARY 2015

Impact Factor: 5.64 · DOI: 10.1021/ac504296e · Source: PubMed

2 AUTHORS, INCLUDING:

Yih-Fan Chen
National Yang Ming University
27 PUBLICATIONS **308** CITATIONS

SEE PROFILE

analytical chemistry

Article

pubs.acs.org/ac

Concentration-Dependent Thermophoretic Accumulation for the Detection of DNA Using DNA-Functionalized Nanoparticles

Li-Hsien Yu[†] and Yih-Fan Chen*[,‡,§,⊥]

[†]Department of Biomedical Engineering, National Cheng Kung University, Tainan 701, Taiwan

[‡]Institute of Biophotonics, National Yang-Ming University, Taipei 112, Taiwan

[§]Biophotonics and Molecular Imaging Research Center, National Yang-Ming University, Taipei 112, Taiwan

[⊥]Medical Device Innovation Center, National Cheng Kung University, Tainan 701, Taiwan

ABSTRACT: Thermophoresis is a phenomenon about the migration of particles along a temperature gradient and is sensitive to the properties of particles and the surrounding medium. While a few studies have investigated its mechanisms and effects on particle motion in recent years, the applications of thermophoresis in biosensing has not been well explored. In this study, we demonstrate a thermophoresis-based method for detecting DNA. We use DNA-functionalized gold nanoparticles and fluorescent DNA probes to capture target DNA in free solution, and we demonstrate that the hybridization between the specially designed capture probes and the target DNA significantly changes the thermophoretic properties of the fluorescent probes. As a result, the target DNA can be specifically detected in serum-containing buffers based on the spatial distribution of the fluorescent probes in a laser-induced temperature gradient. The optical setup consists of only a laser and an epifluorescence microscope, and the detection does not rely on any micro- or nanofabricated devices. In addition, because the detection is based on the thermophoretic motion of molecules in free solution, no capture probes need to be immobilized on a fixed surface before detection, and no channels or pumps are needed for washing away unbound molecules. The thermophoresis-based biosensing method is found to be simple and effective for detecting DNA.

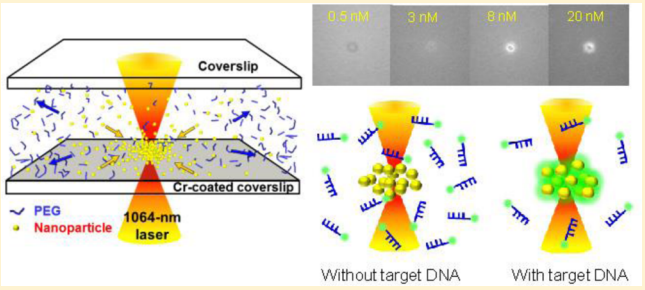

The ability to manipulate flows, molecules, and micro- and nanoparticles is critical to the processing and analysis of biological samples in lab-on-a-chip systems. Various kinds of microfluidic components[1] and techniques based on electrokinetic phenomena, such as capillary electrophoresis (CE),[2] dielectrophoresis (DEP),[3] and electroosmosis,[4] have been developed and widely used by the microfluidic community to separate, transport, concentrate, and mix particles and molecules. For example, optoelectronic tweezers (OET),[5] which is based on light-induced DEP, has been demonstrated as a powerful tool that allows for massively parallel manipulation of cells. In addition to the commonly used electrokinetic techniques, thermophoresis,[6−12] the migration of particles in a temperature gradient, has drawn increasing attention in the past decade because of its ability to move small molecules, such as DNA and proteins, in liquids.

Recent studies have shown that thermophoretic effects can be used to manipulate and analyze particles and molecules in liquids. Braun and Libchaber showed that 5.6 kbp DNA was depleted by thermophoresis at the beginning of laser irradiation and was then accumulated in the hotter region through the interplay of thermophoresis and convection.[13] As reviewed by Duhr and Braun[7] and Piazza,[14] thermophoretic effects are influenced by several factors, including the conformation, size, and charge of the particle, as well as the pH, salt concentration, and temperature of the surrounding medium. Therefore, although thermophoresis usually drives DNA[15−19] and polystyrene beads[12,19−21] away from the hotter regions in commonly used buffer solutions, the sign of the Soret coefficient, which determines the direction of thermophoretic motion, could be reversed by changing the properties of the medium. Jiang et al.,[20] for example, demonstrated that polystyrene beads could be driven toward the hotter regions when the volume fraction of polyethylene glycol (PEG), a kind of polymer, in the solution was higher than a certain level. Their results showed that, as a PEG gradient was built by thermophoretic depletion, polystyrene beads could be accumulated in the hotter regions by thermophoresis. The accumulation of DNA, RNA, and polystyrene beads of different sizes demonstrated the dependence of thermophoresis on particle size.[21] Later studies further showed that not only the size but also the conformation affected the thermophoretic motion of oligonucleotides.[22] The transport and accumulation of DNA could become more efficient when thermophoretic motion and bidirectional flows were combined to create "conveyor belts" in solution.[23] In addition to thermophoretic

Received: November 17, 2014
Accepted: February 3, 2015
Published: February 3, 2015

DOI: 10.1021/ac504296e
Anal. Chem. 2015, 87, 2845−2851

accumulation, thermophoretic depletion of DNA and proteins has also been explored. Because thermophoresis is sensitive to the binding-induced changes in the properties of the molecules, the concentration and binding affinity of molecules can be determined based on the level of thermophoretic depletion.[24−28]

As demonstrated by the studies mentioned above, thermophoresis has drawn increasing attention for its ability to manipulate and analyze molecules. Analyzing biomolecules based on their thermophoretic motion has several advantages. First, because thermophoresis-based methods analyze molecules in free solution directly without using micro- or nanofabricated devices, the accuracy and reproducibility of detection are not affected by the quality of fabrication processes as in the cases of chip-based electrical, optical, and mechanical biosensing methods. Second, unlike many other biosensing methods,[29] thermophoresis-based biosensing does not require immobilization of capture probes, such as antibodies or oligonucleotides, on a fixed sensor surface to capture target molecules and does not need multiple washing steps to remove uncaptured molecules before detection. Therefore, no pumps, tubing, and microchannels are needed for washing the sensor surface, which simplifies the design and operation of the system. The whole system consists of only a fluorescence detection system and a heating source that can be either a laser beam as shown in this study or other types of sources such as an electrode. Third, because thermophoresis-based biosensing does not need to capture target molecules on a fixed sensor surface, reactants can be homogeneously mixed in a test tube before they are put into a flow chamber for detection. In such cases, the binding rate of the capture probes to the target molecules is not limited by mass transport. Finally, because the level of thermophoretic depletion or accumulation is usually determined based on the spatial distribution of the fluorescent molecules[24−28] rather than the absolute fluorescence intensity, the accuracy and reproducibility of detection can be less interfered by autofluorescence from other molecules in solution and changes in fluorescence detection efficiency. Given the advantages mentioned above, thermophoretic depletion has been used to measure the binding affinity and concentration of biomolecules.[24−28] However, the dependence of the levels of thermophoretic depletion on the concentration of the target molecules is usually quite small. If the binding between the capture probes and the target molecules can induce more changes on their thermophoretic motion, the molecules can be detected more accurately using thermophoresis.

In this work, we demonstrated a simple and robust approach to DNA detection using thermophoresis. To increase the dependence of thermophoretic motion on the concentration of the target DNA, we mixed the target DNA with the specially designed capture probes that consisted of fluorescently labeled DNA and DNA-functionalized gold nanoparticles (AuNPs) in a PEG-containing buffer solution before the samples were injected into a flow chamber for detection. As will be detailed later, instead of depletion, we detected the target DNA based on the thermophoretic accumulation of the fluorescent DNA probes. The hybridization between the oligonucleotides significantly changed the speed of the fluorescent DNA's thermophoretic motion and caused an enhancement in the fluorescence in the hotter regions with increasing concentration of the target DNA. In short, we demonstrated for the first time that oligonucleotides can be detected based on the level of the thermophoretic accumulation of fluorescent probes. In addition, our results showed that this new DNA detection method could function well even when the solution contained 10% of fetal bovine serum.

EXPERIMENTAL SECTION

Materials. All oligonucleotides were obtained from MDBio, Inc. The 20 nm AuNPs were purchased from BBI Solutions. Other chemical and biochemical products, including NaCl, Na_2HPO_4, NaH_2PO_4, polyethylene glycol (PEG) 10000, tris(2-carboxyethyl)phosphine (TCEP), Tween 80, phosphate buffer saline (PBS), bovine serum albumin (BSA), Rhodamine B, and fetal bovine serum, were all obtained from Sigma-Aldrich.

Construction of Flow Chambers. To make a flow chamber, two coverslips were bound together by two pieces of double-sided tape, which also served as spacers and boundaries of the chamber. The volume of the flow chamber was ∼3 μL. To enhance light absorption, one of the two coverslips was coated with a 40 nm thick chromium (Cr) layer on one surface, serving as the bottom of the flow chamber. To prevent nonspecific binding on the surfaces of the chamber, the chamber was incubated with PBS buffer containing 0.5% BSA for 10 min prior to experiments.

Optical Setup. Figure 1 is a schematic illustrating the experimental setup. A 1064 nm laser (CNI) was focused by a 20× objective lens with N.A. 0.45 to generate a temperature gradient in the flow chamber. The objective was mounted below a sample stage of an upright epifluorescence microscope (Olympus BX51). Images of samples were captured using a CCD camera (Hamamatsu ORCA R2) and a 20× objective with N.A. 0.75, which was mounted above the sample stage. An optical low-pass filter was installed before the camera port to prevent the laser light from entering the camera.

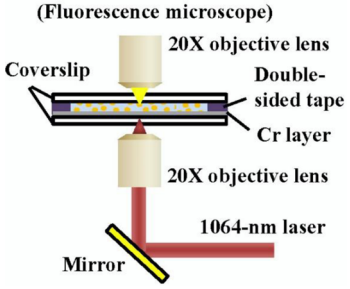

Figure 1. Schematic showing the optical setup used for detecting DNA by thermophoresis. A 1064 nm laser beam was focused by a 20× objective on a Cr layer to create a temperature gradient in a flow chamber made by coverslips and double-sided tape.

Temperature Measurement. Rhodamine B dyes with temperature-dependent quantum yield were used to measure the temperature distribution under laser irradiation. A 50 μM solution of Rhodamine B in 50 mM carbonate buffer was injected into a flow chamber for temperature measurement, and the upright epifluorescence microscope was used to measure the spatial distribution of fluorescence. Given that fluorescence intensity was a function of temperature, the increase in temperature of the solution during laser irradiation was calculated based on the relative change in the fluorescence intensity, as described previously.[30] Briefly, fluorescence images were captured before and after laser irradiation for 5 min. Light from a mercury lamp, which served as an excitation source for fluorescence microscopy, was blocked by a shutter when images

DOI: 10.1021/ac504296e
Anal. Chem. 2015, 87, 2845−2851

were not taken to prevent photobleaching. The image taken after heating was normalized by the image taken at room temperature, and then the normalized fluorescence intensity was substituted into a calibration curve to calculate temperature.

Synthesis of DNA-Functionalized AuNPs. The thiol-modified DNA molecules (see Table 1) were conjugated to AuNPs through gold−thiol chemistry, as previously reported.[31] Briefly, the thiol group of the DNA was activated by 0.l mM TCEP for 1 h at room temperature, and 200 μL of AuNPs were incubated in 0.04% Tween 80 solution for 30 min at room temperature. The excess Tween 80 in the solution of the AuNPs was removed by centrifugation at 9000g for 15 min after incubation, and then the Tween 80 coated-AuNPs were mixed with 10 μL of the activated DNA in 10 mM phosphate buffer (pH 7.4) containing 0.3 M NaCl. The temperature of the mixture was maintained at 55 °C for 5 h for DNA conjugation. Unconjugated DNA molecules were removed by centrifugation at 9000*g* for 15 min and washed with 1× PBS buffer three times. Final AuNP-DNA conjugates were dispersed in 100 μL of 10 mM phosphate buffer (pH 7.4) containing 0.5 M NaCl.

Table 1. Sequences of the DNA Used in This Work[a]

Name	Sequence
Thiol-modified DNA	5' Thiol-C6-AAA AAA AAC ACA ACA CCC AA 3'
FITC-labeled DNA	5' CAC AAC CAA CCC CAA AAA AA-FITC 3'
Target DNA	5' TGG GGT TGG TTG TGT TGG GTG TTG TGT TT 3'
Mutation I	5' TGG GGT TTG TTG TGT TGG GTG TTG TGT TT 3'
Mutation II	5' TGG GGT TGG TTG TGT TGG GTT TTG TGT TT 3'
Mutation III	5' TGG GGT TTG TTG TGT TGG GTT TTG TGT TT 3'

[a]The target DNA can hybridize with the thiol-modified DNA and the FITC-labeled DNA without any mismatches. Mutation I and II are one-base mismatched targets, and Mutation III is a two-base mismatched target. Underlined letters are the mismatched bases.

Measurement of the Thermophoretic Motion of Molecules. To 50 μL of the AuNP-DNA conjugates was added 1 μL of 1 μM FITC-labeled DNA (see Table 1). Then, to 6 μL of the mixture was added 1 μL of a solution that contained a certain concentration of the target DNA (see Table 1). The temperature of the mixture was increased to 70 °C and then was decreased to room temperature in 30 min for DNA hybridization. Then, PEG 10000 was added to the solution to reach a mass fraction of 15%. The mixture was shaken for 10 min before it was used for measurement.

To measure the thermophoretic motion of molecules, the prepared mixture was put in a flow chamber mounted on the sample stage of the optical setup. The 1064 nm laser was focused on the Cr layer of the flow chamber, and the laser power was 8 mW before the objective when obtaining the calibration curves. After laser irradiation for 5 min, a fluorescence image was taken for analysis. The light from the mercury lamp was blocked during laser irradiation to prevent unnecessary photobleaching.

To obtain the calibration curves for the detection of DNA, the experimental steps described above were repeated several times using AuNP-DNA conjugates mixed with various concentrations of the target DNA. In addition, to obtain calibration curves in serum-containing buffers, similar experiments were repeated with samples in solutions containing 10% fetal bovine serum.

To determine the effects of the mass fraction PEG on thermophoresis, samples contained only the capture probes, which were the AuNP-DNA conjugates and the FITC-labeled DNA, and samples contained both the capture probes and the target DNA were prepared. The concentration of the FITC-labeled DNA and the target DNA was 12 nM and 50 nM, respectively. PEG 10000 was added to each prepared mixture to reach a mass fraction ranging between 0% and 15%. Spatial distribution of FITC-DNA after laser irradiation was measured with the samples containing various mass fractions of PEG 10000.

Image Analysis. Images taken during thermophoresis experiments were analyzed using ImageJ. The average intensities of the fluorescence in the colder and the hotter regions were measured respectively to calculate the relative change in fluorescence intensity $\Delta I/I$, which was given by

$$\frac{\Delta I}{I} = \frac{I_{\mathrm{hot}} - I_{\mathrm{cold}}}{I_{\mathrm{cold}}} \quad (1)$$

with I_{hot} the average fluorescence intensity of a circular area (diameter 13 μm) centered at the laser spot and I_{cold} the average fluorescence intensity of a rectangular region (75 × 85 μm) located 20 μm away from the laser.

RESULTS AND DISCUSSION

To understand the relationship between laser power and the temperature gradient generated by the focused laser beam, the spatial distribution of the temperature in the flow chamber at different laser powers were measured using Rhodamine B dyes, the quantum yield of which were highly dependent on temperature.[30,32] As described previously, a sample was placed in a flow chamber made by placing double-sided tape between two coverslips and was observed under an upright epifluorescence microscope during each measurement. The 1064 nm laser beam was focused on the top surface of the Cr layer by the 20× objective placed under the coverslip to create a temperature gradient. By measuring the fluorescence intensity, spatial maps of the temperature around the heated region after laser irradiation for 5 min were obtained,[18,33] as shown in Figure 2a. Figure 2b shows the maximum temperature of the solution irradiated by laser of various powers. For the DNA detection experiments that will be detailed later, the laser power was set to 8 mW before the objective lens to increase the temperature of the solution at the focal point from ∼23 to ∼31 °C. The low temperature rise ensured that biomolecules being detected would not be damaged by heat.

Figure 3a illustrates the detection scheme used in our experiments for the detection of DNA. To allow the concentration of DNA to be determined based on the thermophoretic motion of fluorescent probes, each sample was well mixed with the capture probes that consisted of DNA-functionalized gold nanoparticles (AuNPs) and fluorescein (FITC)-labeled DNA molecules before detection. Although numerous studies have demonstrated nanoparticle-mediated detection of DNA, including fluorescence resonance energy transfer (FRET)-based[34,35] and colorimetric-based[36] methods, to the best of our knowledge, it was the first time that AuNPs were used for thermophoresis-based DNA detection. In this work, the thiol-modified DNA, which was immobilized on 20

DOI: 10.1021/ac504296e
Anal. Chem. 2015, 87, 2845−2851

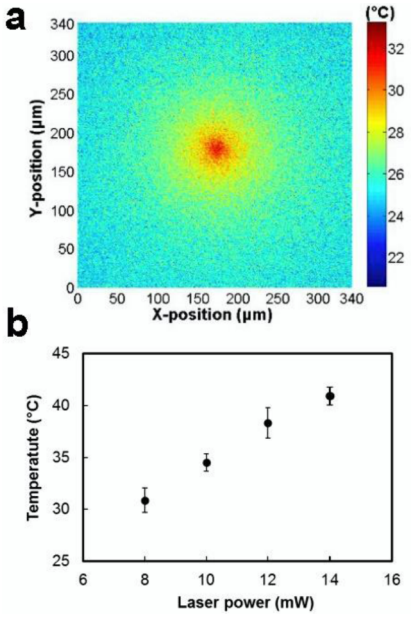

Figure 2. Temperature gradient in solution created by the 1064 nm laser beam focused on the Cr layer of a flow chamber. (b) Spatial map of the temperature around the laser spot after laser irradiation for 5 min. The laser power was 8 mW before the objective when detecting DNA. (c) Maximum temperatures of the solution irradiated by the 1064 nm laser of various powers (n = 5 per power). Error bars, SD.

nm AuNPs, and the FITC-labeled DNA were designed so that they could hybridize with the target DNA to from a sandwiched hybrid, as shown in Figure 3a. The sequences of the thiol-modified DNA, the FITC-labeled DNA, and the target DNA are shown in Table 1. Through DNA hybridization, multiple FITC-labeled DNA molecules could be immobilized on the surface of each AuNP in the presence of the target DNA. By adding some PEG to the solution, we accumulated the AuNPs in the hotter regions by thermophoresis in a laser-induced temperature gradient, as shown in Figure 3b. It should be noted that because the FITC-labeled DNA molecules that were immobilized on the AuNPs via DNA hybridization moved with the AuNPs, the intensity of fluorescence in the hotter regions gradually increased during laser irradiation, as shown in Figure 3c. On the other hand, the FITC-labeled DNA molecules that did not form sandwiched hybrids with the other two kinds of DNA remained roughly evenly distributed in the solution because they were too small to be effectively accumulated by thermophoresis under our experimental conditions (Figure 3c). Figure 3d contains representative images showing the spatial distribution of fluorescence after laser irradiation for 5 min when the concentration of the target DNA was 3 and 50 nM, respectively.

In short, the detection scheme proposed in this study allowed the presence of the target DNA to induce a significant change in the thermophoretic motion of the fluorescent DNA probes. According to the scheme, because the amount of FITC-labeled DNA immobilized on the AuNPs increases with the amount of the target DNA, the accumulation of the FITC-labeled DNA in the hotter regions by thermophoresis is expected to be more prominent when there is more target DNA. As a result, we can detect the target DNA by measuring the relative changes in fluorescence intensity between the hotter and colder regions after laser irradiation, as will be shown later.

To better detect DNA using the proposed thermophoresis-based detection scheme, the thermophoretic motion of the fluorescent DNA probes should change as much as possible when the target DNA molecules hybridize with the capture probes. Given that previous studies have shown that the fraction of PEG can affect the thermophoretic accumulation of polymer beads[20,21] and oligonucleotides,[21,22] we first measured the thermophoretic accumulation of FITC-labeled DNA under various mass fractions of PEG 10 000. We prepared two kinds of samples for the experiments. The first kind of sample contained only the capture probes, which included the FITC-labeled DNA and the DNA-functionalized AuNPs that are described previously, but not the target DNA. The other kind of sample contained both the capture probes and the target DNA, and the concentration of the target DNA was about four

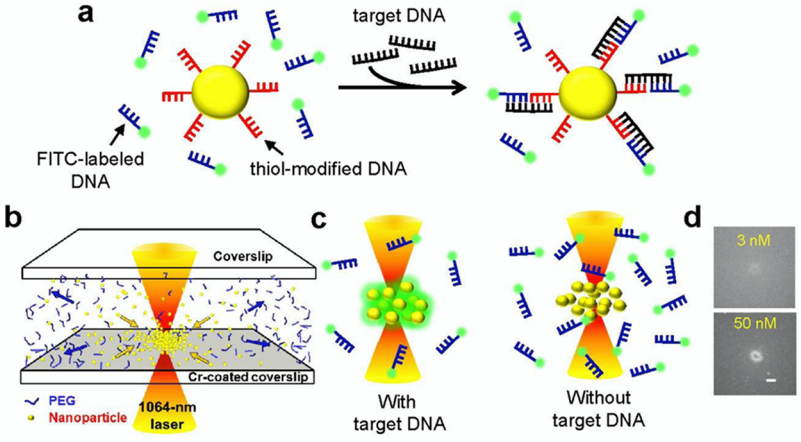

Figure 3. Schematic of the scheme used for detecting DNA by thermophoresis. (a) Schematic showing that when the target DNA is present, the target DNA can hybridize with the thiol-modified DNA and the FITC-labeled DNA to form a sandwiched hybrid. More FITC-labeled DNA is immobilized on the AuNPs when there is more target DNA. (b) Schematic showing that when a small fraction of PEG is present in the solution, the PEG molecules move toward the colder regions during laser irradiation, while the AuNPs move toward the laser focus because of the PEG gradient. The FITC-labeled DNA that is immobilized on the AuNPs via DNA hybridization moves with the AuNPs. (c) Schematic showing that the amount of the FITC-labeled DNA accumulated in the hotter regions varies with the amount of the target DNA. (d) Representative images showing the spatial distribution of fluorescence of two samples with 3 nM and 50 nM of the target DNA, respectively. Scale bar, 10 μm.

DOI: 10.1021/ac504296e
Anal. Chem. 2015, 87, 2845−2851

times higher than that of the capture probes to ensure that a significant portion of the FITC-labeled DNA molecules were immobilized on the AuNPs. For each of the two kinds of samples, we observed the spatial distribution of fluorescence after irradiating the solution with an 8 mW 1064 nm laser for 5 min. Then, the relative change in fluorescence intensity $\Delta I/I$ was calculated as described previously.

Figure 4a shows that after laser irradiation, the spatial distribution of fluorescence changed with the mass fraction of PEG for the samples that contained target DNA, whereas the spatial distribution of fluorescence was almost the same for the samples with various mass fractions of PEG when there was no target DNA in the samples. As shown in Figure 4b, $\Delta I/I$ was small for both target-containing and nontarget-containing samples when there was no PEG in the buffer solution. However, when the mass fraction of PEG was increased from 0% to 15%, $\Delta I/I$ of the target-containing samples significantly increased with the mass fraction of PEG, but $\Delta I/I$ of the nontarget-containing samples remained small overall. From the results of the experiments, we found that among the mass fractions of PEG tested, the samples with 15% PEG showed the largest difference in $\Delta I/I$ between target-containing and nontarget containing samples. Therefore, we used buffers that contained 15% PEG for the following experiments. We did not perform experiments with buffer solutions that contained more than 15% PEG because the solution would become too viscous.

During the detection process, we irradiated each sample with a focused 1064 nm laser beam for 5 min and then took an image of the sample under an epifluorescence microscope to record the spatial distribution of the FITC-labeled DNA, which had moved in the laser-induced temperature gradient because of thermophoresis. To obtain calibration curves for DNA detection, we performed experiments with samples that contained the same amount of the capture probes but different concentrations of the target DNA. In addition, to understand whether the detection method can be used to detect DNA in complex biological liquids, the measurements were done in pure phosphate buffers and in phosphate buffers that contained 10% fetal bovine serum, respectively. In both cases, the buffer solutions contained 15% PEG 10 000 so that the DNA-functionalized AuNPs could be accumulated by thermophoresis. As shown in Figure 5a,b, the amount of the FITC-DNA accumulated in the hotter regions increased with the increasing concentration of the target DNA, as expected from the detection scheme. As explained previously, when more target DNA molecules were present, more FITC-DNA molecules could be immobilized on the surfaces of the AuNPs through DNA hybridization. Consequently, when AuNPs moved to the hotter regions because of thermophoresis, the samples that contained more target DNA molecules showed stronger fluorescence around the laser spot. The two calibration curves, for the samples in pure buffers and in serum-containing buffers respectively, are shown in Figure 5c. When the samples were in

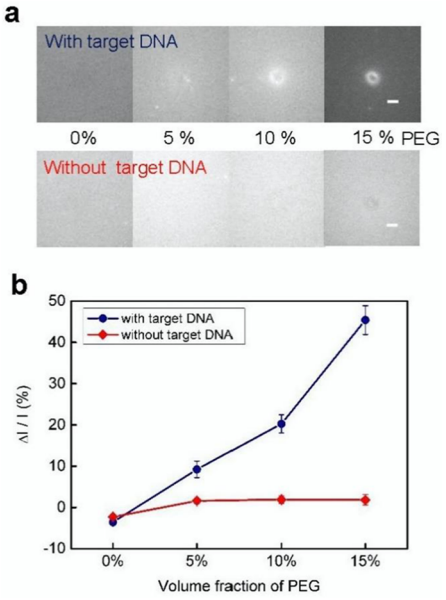

Figure 4. Effects of the mass fraction of PEG on the spatial distribution of fluorescence after samples containing the synthesized capture probes were irradiated by a focused laser beam for 5 min. (a) Representative images showing the spatial distribution of fluorescence for target-containing and nontarget-containing samples with various mass fractions of PEG. Scale bars, 10 μm. (b) Calculated $\Delta I/I$ for target-containing (blue solid circle) and nontarget-containing (red solid diamond) samples with various mass fractions of PEG (n = 6 per experimental condition). Error bars, SD.

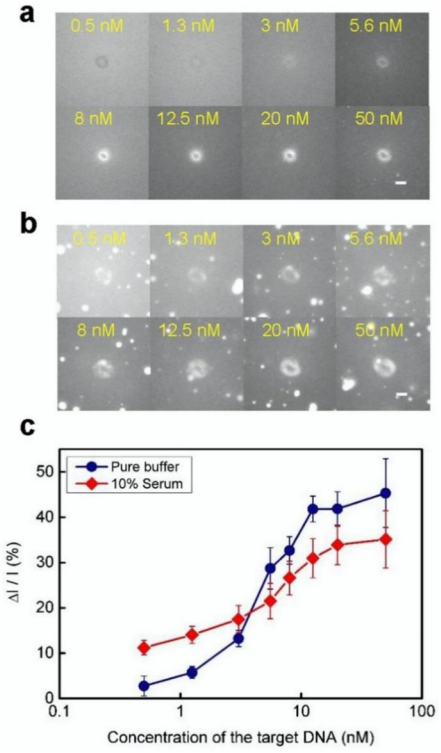

Figure 5. Detecting DNA based on the relative change in fluorescence intensity around the laser focus after samples containing the synthesized capture probes and the target DNA were irradiated by a focused laser beam for 5 min. (a,b) Representative images showing that the spatial distribution of fluorescence after laser irradiation was dependent on the concentration of the target DNA. The results were obtained from samples in (a) pure phosphate buffers and in (b) phosphate buffers that contained 10% fetal bovine serum. Scale bars, 10 μm. (c) $\Delta I/I$ for samples with various concentrations of the target DNA (n = 12 per experimental condition). The results were obtained with samples in pure phosphate buffers (solid blue circle) and in phosphate buffers that contained 10% fetal bovine serum (solid red diamond), respectively. Error bars, SD.

DOI: 10.1021/ac504296e
Anal. Chem. 2015, 87, 2845−2851

pure phosphate buffers, $\Delta I/I$ increased from ~0% to ~42% as the concentration of the target DNA increased from 0.5 to 50 nM. While the calibration curve obtained in the serum-containing buffers was slightly different from that obtained in the pure buffer solutions, $\Delta I/I$ still increased with the target DNA. The differences between the two calibration curves might be caused by the competitive binding of the target DNA and the proteins in serum with the capture probes, the autofluorescence of the proteins in serum, or the changes in the properties of fluids such as pH, viscosity, and salt concentration.[24,25] Yet, our results demonstrate that the concentration of the target DNA can be determined based on the spatial distribution of the fluorescent probes under a temperature gradient, even when the sample is from complex biological liquids, such as serum.

To verify that the detection of DNA is sequence-specific, we performed experiments with samples that had either single-base mismatched or two-base mismatched target DNA in addition to the fully matched target DNA. The concentration of the matched or the mismatched target DNA in each sample was 50 nM, and the sequences of the mismatched target DNA are shown in Table 1. As illustrated in Figure 6a,b, $\Delta I/I$ of the

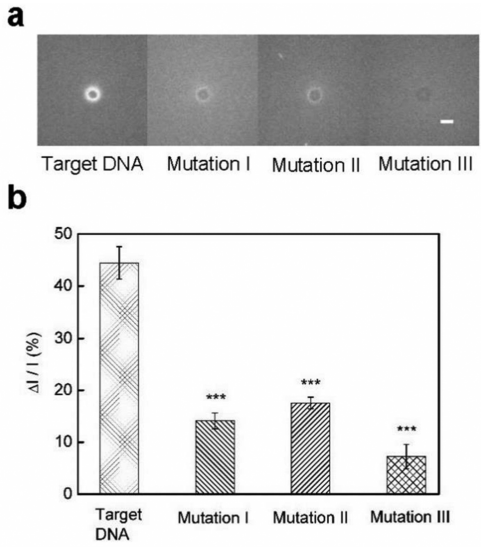

Figure 6. Verifying the detection of DNA was sequence-specific. Samples containing the synthesized capture probes and either the target DNA or the mismatched target DNA were irradiated by a focused laser beam for 5 min. (a) Representative images showing that the increase in the fluorescence intensity around the laser focus was more prominent when the samples contained the target DNA rather than the single-base mismatched (Mutation I and II) or two-base mismatched (Mutation III) target DNA. Scale bar, 10 μm. (b) $\Delta I/I$ for samples with 50 nM of the target DNA, Mutation I, II, and III, respectively (n = 6 per kind of DNA, ***p < 0.001). Error bars, SD.

samples containing the mismatched target DNA, namely Mutation I, II, and III, was much lower than that of the samples with the fully matched target DNA. The samples with Mutation III, namely the two-base mismatched target DNA, showed the lowest $\Delta I/I$, as expected. The results show that the detection of DNA is indeed sequence-specific.

CONCLUSIONS

We have demonstrated a thermophoresis-based biosensing method that allows for the detection of DNA by observing the thermophoretic accumulation of fluorescent DNA probes around a laser focus. When using the proposed detection scheme, the amount of the fluorescent probes accumulated by thermophoresis increases with the amount of the target DNA, and the level of the accumulation of fluorescent probes can be determined by simple image analysis.

The whole biosensing system consists of only a fluorescence detection system and a heating source, which is a laser beam in this study but can also be other types of sources such as an electrode. All reagents can be well mixed in a test tube before detection, so the binding between the target molecules and the capture probes is not limited by mass transport. In addition, because the target DNA is detected in free solution directly, the surfaces of the flow chambers do not need to be functionalized with capture probes, and the system does not need tubing and pumps for washing away molecules that are not captured by the probes. The detection is conducted without any micro- or nanofabricated chip, and sample solution can be just put in capillary tubes or flow chambers made by coverslips and double-sided tape for detection. The detection process involves only heating for no more than 5 min and capturing a fluorescence image. The whole system is very simple and easy to operate, and the detection is sequence-specific and resistant to the interference from the molecules and proteins in serum. To our knowledge, this biosensing method is the first thermophoresis-based DNA detection method.

In short, this study demonstrates a new biosensing method based on thermophoresis, which is sensitive to the molecular binding-induced changes in the properties of the molecules. Although thermophoresis has been used to measure antibody concentration and affinity in other studies,[24−28] the new sensing scheme uses gold nanoparticles, which can be accumulated by thermophoresis much more quickly than the fluorescent probes, to increase the change in thermophoretic accumulation with the concentration of the target molecules. The sensitivity of the detection can be improved by optimizing the experimental parameters such as the number of DNA probes immobilized on each nanoparticle and the number of nanoparticles used in detection. In addition, besides DNA detection, the sensing scheme can be modified for the detection of proteins and other molecules by using DNA aptamers in the scheme. We envisage that the rapid and simple thermophoresis-based detection method can be utilized in many biosensing applications such as disease detection.

AUTHOR INFORMATION

Corresponding Author

*Y.-F. Chen. E-mail: chenyf@ym.edu.tw.

Author Contributions

The paper was written through contributions of all authors. All authors have given approval to the final version of the paper.

Notes

The authors declare no competing financial interest.

ACKNOWLEDGMENTS

We gratefully acknowledge the financial support from the Ministry of Science and Technology (NSC 101-2627-E-002-003, MOST 103-2221-E-010-007-MY3), the Biophotonics and Molecular Imaging Research Center at the National Yang-Ming University, and the Medical Device Innovation Center at the National Cheng Kung University. We also thank C. K. Lee, C. T. Lin, Y. S. Hsu, N. Z. Huang (National Taiwan University), S.

DOI: 10.1021/ac504296e
Anal. Chem. 2015, 87, 2845−2851

Y. Lee (Tamkang University), and S. S. Lee (National Taiwan Ocean University) for discussions and comments on the designs of the experiments.

REFERENCES

(1) Squires, T. M.; Quake, S. R. *Rev. Mod. Phys.* **2005**, *77*, 977−1026.
(2) Harrison, D. J.; Manz, A.; Fan, Z. H.; Ludi, H.; Widmer, H. M. *Anal. Chem.* **1992**, *64*, 1926−1932.
(3) Pohl, H. A. *J. Appl. Phys.* **1951**, *22*, 869−871.
(4) Glasgow, I.; Batton, J.; Aubry, N. *Lab Chip* **2004**, *4*, 558−562.
(5) Chiou, P. Y.; Ohta, A. T.; Wu, M. C. *Nature* **2005**, *436*, 370−372.
(6) Parola, A.; Piazza, R. *Eur. Phys. J. E: Soft Matter Biol. Phys.* **2004**, *15*, 255−263.
(7) Duhr, S.; Braun, D. *Proc. Natl. Acad. Sci. U. S. A.* **2006**, *103*, 19678−19682.
(8) Wurger, A. *Phys. Rev. Lett.* **2007**, *98*, 138301.
(9) Piazza, R.; Parola, A. *J. Phys.: Condens. Matter* **2008**, *20*, 153102.
(10) Wurger, A. *Rep. Prog. Phys.* **2010**, *73*, 126601.
(11) Weinert, F. M.; Mast, C. B.; Braun, D. *Phys. Chem. Chem. Phys.* **2011**, *13*, 9918−9928.
(12) Braun, M.; Cichos, F. *ACS Nano* **2013**, *7*, 11200−11208.
(13) Braun, D.; Libchaber, A. *Phys. Rev. Lett.* **2002**, *89*, 188103.
(14) Piazza, R. *Soft Matter* **2008**, *4*, 1740−1744.
(15) Duhr, S.; Braun, D. *Phys. Rev. Lett.* **2006**, *97*, 038103.
(16) Jiang, H. R.; Sano, M. *Appl. Phys. Lett.* **2007**, *91*, 154104.
(17) Reineck, P.; Wienken, C. J.; Braun, D. *Electrophoresis* **2010**, *31*, 279−286.
(18) Serey, X.; Mandal, S.; Chen, Y. F.; Erickson, D. *Phys. Rev. Lett.* **2012**, *108*, 048102.
(19) Reichl, M. R.; Braun, D. *J. Am. Chem. Soc.* **2014**, *136*, 15955−15960.
(20) Jiang, H.-R.; Wada, H.; Yoshinaga, N.; Sano, M. *Phys. Rev. Lett.* **2009**, *102*, 208301.
(21) Maeda, Y. T.; Buguin, A.; Libchaber, A. *Phys. Rev. Lett.* **2011**, *107*, 038301.
(22) Maeda, Y. T.; Tlusty, T.; Libchaber, A. *Proc. Natl. Acad. Sci. U. S. A.* **2012**, *109*, 17972−17977.
(23) Weinert, F. M.; Braun, D. *Nano Lett.* **2009**, *9*, 4264−4267.
(24) Baaske, P.; Wienken, C. J.; Reineck, P.; Duhr, S.; Braun, D. *Angew. Chem., Int. Ed.* **2010**, *49*, 2238−2241.
(25) Wienken, C. J.; Baaske, P.; Rothbauer, U.; Braun, D.; Duhr, S. *Nat. Commun.* **2010**, *1*, 100.
(26) Lippok, S.; Seidel, S. A. I.; Duhr, S.; Uhland, K.; Holthoff, H. P.; Jenne, D.; Braun, D. *Anal. Chem.* **2012**, *84*, 3523−3530.
(27) Seidel, S. A.; Wienken, C. J.; Geissler, S.; Jerabek-Willemsen, M.; Duhr, S.; Reiter, A.; Trauner, D.; Braun, D.; Baaske, P. *Angew. Chem., Int. Ed.* **2012**, *51*, 10656−10659.
(28) Seidel, S. A.; Markwardt, N. A.; Lanzmich, S. A.; Braun, D. *Angew. Chem., Int. Ed.* **2014**, *53*, 7948−7951.
(29) Turner, A. P. F. *Chem. Soc. Rev.* **2013**, *42*, 3184−3196.
(30) Samy, R.; Glawdel, T.; Ren, C. L. *Anal. Chem.* **2008**, *80*, 369−375.
(31) Xu, S. M.; Yuan, H.; Xu, A.; Wang, J.; Wu, L. J. *Langmuir* **2011**, *27*, 13629−13634.
(32) Erickson, D.; Sinton, D.; Li, D. Q. *Lab Chip* **2003**, *3*, 141−149.
(33) Cordero, M. L.; Verneuil, E.; Gallaire, F.; Baroud, C. N. *Phys. Rev. E* **2009**, *79*, 011201.
(34) Zhang, C. Y.; Yeh, H. C.; Kuroki, M. T.; Wang, T. H. *Nat. Mater.* **2005**, *4*, 826−831.
(35) Cheng, Y.; Stakenborg, T.; Van Dorpe, P.; Lagae, L.; Wang, M.; Chen, H.; Borghs, G. *Anal. Chem.* **2011**, *83*, 1307−1314.
(36) Xia, F.; Zuo, X. L.; Yang, R. Q.; Xiao, Y.; Kang, D.; Vallee-Belisle, A.; Gong, X.; Yuen, J. D.; Hsu, B. B. Y.; Heeger, A. J.; Plaxco, K. W. *Proc. Natl. Acad. Sci. U. S. A.* **2010**, *107*, 10837−10841.

DOI: 10.1021/ac504296e
Anal. Chem. 2015, 87, 2845−2851